JOURNAL OF THERMOPHYSICS AND HEAT TRANSFER
Vol. 18, No. 2, April–June 2004

Radiative Heat Transfer Solutions for Anisotropically Scattering Media: The Use of Wavelets

Oguzhan Guven* and Yildiz Bayazitoglu†
Rice University, Houston, Texas 77005

Wavelet analysis is presented for solving the radiative transfer problem for a scattering media. The governing equations are shown to reduce to a system of first-order ordinary differential equations. The presented solution is applicable to any square integrable scattering phase function. A one-dimensional plane-parallel geometry is chosen, and a linearly anisotropic scattering medium is assumed to compare the solution with the results of the previous research.

Nomenclature

$A_{i,j}$, B_i	=	bookkeeping matrices
a_i, b_i	=	wavelet expansion coefficients
$f(t)$	=	square integrable function
h_n	=	wavelet coefficients
I	=	radiative intensity
I_b	=	blackbody intensity
N	=	number of wavelet expansion coefficients
q	=	heat flux
$S_{i,j}$	=	bookkeeping matrices
T	=	temperature
t	=	independent parameter
W_i	=	wrapped around wavelet basis
α	=	linear anisotropic scattering phase function coefficient
δ	=	kronecker δ function
θ	=	polar angle
κ	=	absorption coefficient
μ	=	directional cosine $= \cos\theta$
σ	=	scattering coefficient
σ_{SB}	=	Stefan–Boltzmann constant
τ	=	optical thickness
Φ	=	scattering phase function
φ	=	dilation function
ψ	=	wavelet function
Ω	=	solid angle
ω	=	albedo

Subscripts

L	=	distance between the plates
1, 2	=	left and right walls

Superscripts

$+, -$	=	positive and negative directions
$'$	=	incoming direction

Introduction

THE wavelet analysis[1,2] is applied to the solution of the radiative transfer equation for an anisotropically scattering medium. A one-dimensional medium is chosen, and a linearly anisotropic medium is assumed to compare with the solutions presented in previous work.[3–5]

To construct a wavelet function ψ, Daubechies[6] started from the dilation equation for the scaling function φ,

$$\varphi(t) = \sum_n h_n \varphi_{-1,n} = \sqrt{2} \sum_n h_n \varphi(2t - n), \quad n = 0, \ldots, N-1 \tag{1}$$

and found that the wavelet function satisfies a similar dilation equation,

$$\psi(t) = \sqrt{2} \sum_n (-1)^{n-1} h_{N-n-1} \varphi(2t - n), \quad n = 0, \ldots, N-1 \tag{2}$$

More important, a set of h_n coefficients, up to $N = 20$ (where N has to be even), are constructed. Because φ and ψ have finite supports, that is, they only have nonzero values in a finite interval, they are calculated numerically. Daubechies[6] proved that wavelets construct a set of orthogonal basis for the L^2 function space and gave a detailed construction procedure for these wavelets, and Mallat[7] developed the computational algorithm.

Newland[8] gave a wavelet series expansion of the L^2 function $f(t)$ as follows:

$$f(t) = b_0 + \sum_j \sum_k b_{2^j+k} W(2^j t - k)$$

$$0 \le t < 1, \qquad j = 0, \infty \qquad k = 0, 2^j - 1 \tag{3}$$

where $W(2^j t - k)$ are the Daubechies wavelets confined in the interval $0 \le t < 1$ and wrapped around the interval $0 \le t < 1$ as many times as necessary to ensure that their entire length is included in this interval. Therefore, outside of this interval, these wrapped around wavelets vanish to zero. The inner product of any single wavelet or any two distinct wavelets from the same family is identically zero. These orthogonality properties are expressed as

$$\int_0^1 W(2^j t - k) W(2^{j'} t - k') \, \mathrm{d}t = \delta_{jj'} \delta_{kk'} \tag{4a}$$

$$\int_0^1 W(2^j t - k) \, \mathrm{d}t = 0 \tag{4b}$$

where δ is the Kronecker δ function. The general coefficients can be calculated by taking the inner product of the function and the wavelet basis as

$$b_0 = \int_0^1 f(t) \, \mathrm{d}t \tag{5a}$$

Received 27 January 2003; revision received 22 July 2003; accepted for publication 5 September 2003.

*Graduate Student, Department of Mechanical Engineering and Materials Science.

†H. S. Cameron Chair Professor, Department of Mechanical Engineering and Materials Science; bayaz@rice.edu. Member AIAA.

$$b_{2^j+k} = \int_0^1 f(t)W(2^j t - k)\,\mathrm{d}t \tag{5b}$$

Mallat[7] and Newland[8] have developed a very efficient algorithm to compute the discrete wavelet transform [Eq. (5)] from sampling points of the function. The wavelets are calculated numerically from the inverse discrete wavelet transform.

The following notation of wavelets is used in this work to simplify the equations:

$$W_1 = 1, \qquad W_i = 2^{j/2}\cdot W(2^j t - k), \qquad i = 2, 3, \ldots, N \tag{6}$$

where $i = 2^j + k + 1$ and $k = 0, 1, \ldots, 2^j - 1$. Here j and k are integers and describe the scaling and dilation of the wavelets, respectively.

In this study, the wavelet basis functions are introduced into the radiative transfer equation in the directional domain. This results in a system of ordinary differential equations, which can be solved by several conventional methods.

Analysis

The equation of transfer for azimuthally symmetric radiation in a scattering gray medium within a one-dimensional, plane-parallel medium is[9]

$$\mu\frac{\partial I(\tau,\mu)}{\partial\tau} = I(\tau,\mu) + (1-\omega)I_b + \frac{\omega}{2}\int_{-1}^{1}\Phi(\mu,\mu')I(\tau,\mu')\,\mathrm{d}\mu' \tag{7}$$

where $I(\tau,\mu)$ is the total intensity at optical distance τ in the direction $\mu = \cos\theta$ (Fig. 1). $I(\tau,\mu)\in L^2(R)$ is bounded in the angular domain. The optical distance τ is defined as $\mathrm{d}\tau = (\sigma+\kappa)\,\mathrm{d}x$, where x is the distance. The parameter $\Phi(\mu,\mu')$ is the scattering phase function for azimuthally symmetric radiation. Single scattering albedo is defined as

$$\omega = \sigma/(\sigma+\kappa) \tag{8}$$

In the case of pure scattering, the value of $\omega = 1$, and for a nonscattering medium, $\omega = 0$.

Wavelet analysis is introduced by splitting the angular domain (represented by directional cosine μ) into two parts, $0 \le \mu < 1$ and $-1 \le \mu < 0$. Then Eq. (7) becomes

$$\mu\frac{\partial I^+(\tau,\mu)}{\partial\tau} = I^+(\tau,\mu) + (1-\omega)I_b(\tau) + \frac{\omega}{2}\int_{-1}^{1}\Phi(\mu,\mu')I(\tau,\mu')\,\mathrm{d}\mu' \tag{9a}$$

$$-\mu\frac{\partial I^-(\tau,\mu)}{\partial\tau} = I^-(\tau,\mu) + (1-\omega)I_b(\tau) + \frac{\omega}{2}\int_{-1}^{1}\Phi(\mu,\mu')I(\tau,\mu')\,\mathrm{d}\mu' \tag{9b}$$

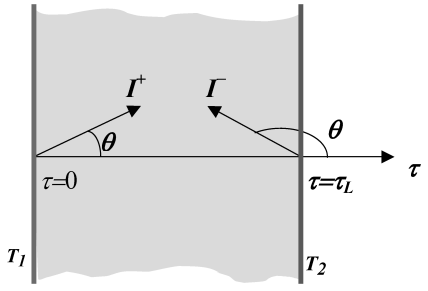

Fig. 1 One-dimensional system geometry.

where $0 \le \mu < 1$ for both equations. Now, we rearrange Eqs. (9a) and (9b) to express the integration in terms of I^+ and I^-,

$$\mu\frac{\partial I^+}{\partial\tau} = I^+ + (1-\omega)I_b + \frac{\omega}{2}\left[\int_0^1\Phi(\mu,-\mu')I^-(x,\mu')\,\mathrm{d}\mu' + \int_0^1\Phi(\mu,\mu')I^+(\tau,\mu')\,\mathrm{d}\mu'\right] \tag{10a}$$

$$-\mu\frac{\partial I^-}{\partial\tau} = I^- + (1-\omega)I_b + \frac{\omega}{2}\left[\int_0^1\Phi(-\mu,-\mu')I^-(x,\mu')\,\mathrm{d}\mu' + \int_0^1\Phi(-\mu,\mu')I^+(\tau,\mu')\,\mathrm{d}\mu'\right] \tag{10b}$$

The method presented in this paper involves approximating positive and negative intensities, I^+ and I^-, in the angular domain by extending them into their wavelet basis,

$$I^+(\tau,\mu) = \sum_{i=1}^{N} a_i(\tau)W_i(\mu) \tag{11a}$$

$$I^-(\tau,\mu) = \sum_{i=1}^{N} b_i(\tau)W_i(\mu) \tag{11b}$$

Introducing preceding expansions into Eqs. (10), we obtain

$$\mu\frac{\partial}{\partial\tau}\sum_i a_i(\tau)W_i(\mu) = \sum_i a_i(\tau)W_i(\mu) + (1-\omega)I_b + \frac{\omega}{2}\sum_i\left[b_i(\tau)\int_0^1\Phi(\mu,-\mu')W_i(\mu')\,\mathrm{d}\mu' + a_i(\tau)\int_0^1\Phi(\mu,\mu')W_i(\mu')\,\mathrm{d}\mu'\right] \tag{12a}$$

$$-\mu\frac{\partial}{\partial\tau}\sum_i b_i(\tau)W_i(\mu) = \sum_i b_i(\tau)W_i(\mu) + (1-\omega)I_b + \frac{\omega}{2}\sum_i\left[b_i(\tau)\int_0^1\Phi(-\mu,-\mu')W_i(\mu')\,\mathrm{d}\mu' + a_i(\tau)\int_0^1\Phi(-\mu,\mu')W_i(\mu')\,\mathrm{d}\mu'\right] \tag{12b}$$

We apply the Galerkin method such that Eqs. (12) are integrated in the angular domain after multiplying by an individual wavelet W_j on both sides:

$$\sum_i\int_0^1\mu W_j(\mu)W_i(\mu)\,\mathrm{d}\mu\frac{\partial a_i}{\partial\tau} = \sum_i a_i\int_0^1 W_j(\mu)W_i(\mu)\,\mathrm{d}\mu + (1-\omega)I_b\int_0^1 W_j(\mu)\,\mathrm{d}\mu + \frac{\omega}{2}\sum_i\left[b_i\int_0^1\int_0^1\Phi(\mu,-\mu')W_j(\mu)W_i(\mu')\,\mathrm{d}\mu'\,\mathrm{d}\mu + a_i\int_0^1\int_0^1\Phi(\mu,\mu')W_j(\mu)W_i(\mu')\,\mathrm{d}\mu'\,\mathrm{d}\mu\right] \tag{13a}$$

$$-\sum_i \int_0^1 \mu W_j(\mu) W_i(\mu)\,\mathrm{d}\mu \frac{\partial b_i}{\partial \tau} = \sum_i b_i \int_0^1 W_j(\mu) W_i(\mu)\,\mathrm{d}\mu + (1-\omega) I_b \int_0^1 W_j(\mu)\,\mathrm{d}\mu + \frac{\omega}{2}\sum_i \left[b_i \int_0^1 \int_0^1 \Phi(-\mu, -\mu') W_j(\mu) W_i(\mu')\,\mathrm{d}\mu'\,\mathrm{d}\mu + a_i \int_0^1 \int_0^1 \Phi(-\mu, \mu') W_j(\mu) W_i(\mu')\,\mathrm{d}\mu'\,\mathrm{d}\mu \right] \quad (13b)$$

When the orthogonality condition of Daubechies' wavelets

$$\int_0^1 W_j(\mu) W_i(\mu)\,\mathrm{d}\mu = \delta_{i,j}, \qquad j = 1, \ldots, N \quad (14a)$$

$$\int_0^1 W_j(\mu)\,\mathrm{d}\mu = \delta_{j,1}, \qquad j = 1, \ldots, N \quad (14b)$$

is utilized and the following bookkeeping notation

$$A_{i,j} = \int_0^1 \mu W_i(\mu) W_j(\mu)\,\mathrm{d}\mu, \qquad i, j = 1, \ldots, N \quad (15a)$$

$$S^1_{i,j} = \int_0^1 \int_0^1 \Phi(\mu, \mu') W_j(\mu) W_i(\mu')\,\mathrm{d}\mu'\,\mathrm{d}\mu \qquad i, j = 1, \ldots, N \quad (15b)$$

$$S^2_{i,j} = \int_0^1 \int_0^1 \Phi(\mu, -\mu') W_j(\mu) W_i(\mu')\,\mathrm{d}\mu'\,\mathrm{d}\mu \qquad i, j = 1, \ldots, N \quad (15c)$$

$$S^3_{i,j} = \int_0^1 \int_0^1 \Phi(-\mu, \mu') W_j(\mu) W_i(\mu')\,\mathrm{d}\mu'\,\mathrm{d}\mu \qquad i, j = 1, \ldots, N \quad (15d)$$

$$S^4_{i,j} = \int_0^1 \int_0^1 \Phi(-\mu, -\mu') W_j(\mu) W_i(\mu')\,\mathrm{d}\mu'\,\mathrm{d}\mu \qquad i, j = 1, \ldots, N \quad (15e)$$

is introduced, Eqs. (12a) and (12b) can be converted to the following compact forms:

$$\sum_i A_{i,j} \frac{\partial a_i(\tau)}{\partial \tau} = a_j(\tau) + (1-\omega) I_b(\tau) \delta_{j,1} + \frac{\omega}{2}\sum_i \left[a_i(\tau) S^1_{i,j} + b_i(\tau) S^2_{i,j} \right] \quad (16a)$$

$$-\sum_i A_{i,j} \frac{\partial b_i(\tau)}{\partial \tau} = b_j(\tau) + (1-\omega) I_b(\tau) \delta_{j,1} + \frac{\omega}{2}\sum_i \left[a_i(\tau) S^3_{i,j} + b_i(\tau) S^4_{i,j} \right] \quad (16b)$$

Equations (16a) and (16b) have $2N$ unknowns, a_i and b_i, where $i, j = 1, \ldots, N$. The system of ordinary differential equations presented in Eqs. (16a) and (16b) can be solved with proper boundary conditions.

To demonstrate the role of wavelets in the current analysis, we choose the simplest boundary conditions, that is, the black walls with constant temperatures at T_1 and T_2: at $\tau = 0$,

$$I^+ = I_b(T_1) \quad (17a)$$

and at $\tau = \tau_L$,

$$I^- = I_b(T_2) \quad (17b)$$

It turns out that the boundary conditions in terms of wavelet expansion coefficients can be obtained by applying the Galerkin method to Eqs. (17) and taking advantage of orthogonality properties of the Daubechies[6] wavelets; at $\tau = 0$,

$$a_j(0) = I_b(T_1)\delta_{j,1}, \qquad j = 1, \ldots, N \quad (18a)$$

and at $\tau = \tau_L$,

$$b_j(\tau_L) = I_b(T_2)\delta_{j,1}, \qquad j = 1, \ldots, N \quad (18b)$$

The most commonly used scattering phase function Φ is the isotropic phase function, which means that $\Phi \equiv 1$. It is the simplest possible phase function. For scattering theories such as Rayleigh scattering and Mie scattering (see Ref. 10), the isotropic phase function model is relatively poor. In this work, we use a linear anisotropic scattering phase function model,

$$\Phi(\mu, \mu') = 1 + \alpha \mu \mu' \quad (19)$$

The coefficient α represents different scattering media. When Eq. (19) is substituted into Eqs. (15b–15e), the bookkeeping matrices for anisotropic scattering become

$$S^1_{i,j} = \delta_{i,1}\delta_{j,1} + \alpha B_i B_j \quad (20a)$$

$$S^2_{i,j} = \delta_{i,1}\delta_{j,1} - \alpha B_i B_j \quad (20b)$$

$$S^3_{i,j} = \delta_{i,1}\delta_{j,1} - \alpha B_i B_j \quad (20c)$$

$$S^4_{i,j} = \delta_{i,1}\delta_{j,1} + \alpha B_i B_j \quad (20d)$$

where

$$B_j = \int_0^1 \mu W_j(\mu)\,\mathrm{d}\mu \quad (21)$$

Notice that Eqs. (16) can be solved with an arbitrary scattering phase function model provided that it is square integrable. This is always true for the real physical situations.

The overall heat flux at optical distance τ is

$$q(\tau) = \int_{4\pi} \hat{\Omega} \cdot I(\tau, \hat{\Omega})\,\mathrm{d}\Omega = 2\pi \sum_{i=1}^{N} [a_i(\tau) - b_i(\tau)] B_i \quad (22)$$

Equations (16) and (18) complete the one-dimensional boundary value problem. The solution algorithm used here to solve the system of ordinary differential equations is the method of particular solutions.[11]

Results

To illustrate the accuracy and the effectiveness of the wavelet method, we solve the problem of radiation transfer in a plane-parallel slab. The medium is emitting, absorbing, and scattering, and the boundaries are black. The left wall is hot, whereas the right one is kept cold. To compare the results with prior researchers,[3,4,12] various α values, including the backward and the forward scattering conditions, are considered. The results obtained with a spatially dependent albedo are presented.

The intensity field results produced by the wavelet method are plotted in Fig. 2. The three profiles in Fig. 2 represent the wavelet approximations of the intensity fields at the midpoint of the spatial domain, $\tau_L/2$, for nonscattering ($\omega = 0$), forward scattering ($\omega = 0.5$ and $\alpha = 1.98398$), and backward scattering ($\omega = 0.5$ and $\alpha = -0.56524$) media. The errors in the approximate intensity field for the nonscattering medium as compared with the exact solution[9] at polar angles $\theta = 0$, 51.7553, 81.7843, and 159.4713 deg are 0.53, 0.72, 0.32, and 1.79%, respectively. This indicates that the present

Table 1 Heat flux comparison: $\tau_L = 1$ and $\omega = 0.8$

	Phase function					
	1, $\alpha = 0.64383$		2, $\alpha = 2.31946$		3, $\alpha = 2.60284$	
Methods	$q(0)$	$q(1)$	$q(0)$	$q(1)$	$q(0)$	$q(1)$
F_9 (exact)	0.76057	0.45588	0.90706	0.60251	0.94178	0.63874
Schuster–Schwarzchild	0.74265	0.42256	0.92518	0.59763	0.95925	0.63069
Two flux	0.7547	0.47124	0.93134	0.64003	0.96279	0.67078
P_1	0.78743	0.46513	0.94485	0.61671	0.98025	0.6511
P_3	0.7659	0.45636	0.91225	0.59739	0.94477	0.62899
P_9 (9 term)	0.76143	0.45637	0.9081	0.60296	0.94297	0.6391
DP_1	0.7587	0.4543	0.9019	0.5923	0.9336	0.6231
Wavelet	0.7617	0.4587	0.9081	0.5991	0.944	0.6344
	% Errors compared to exact results					
Schuster–Schwarzchild	2.356128	7.308941	1.997663	0.809945	1.854998	1.260294
Two flux	0.77179	3.369308	2.67678	6.227283	2.230882	5.016125
P_1	3.531562	2.029043	4.166207	2.356807	4.084818	1.93506
P_3	0.70079	0.105291	0.572178	0.849778	0.317484	1.526443
P_9 (9 term)	0.113073	0.107484	0.114656	0.074688	0.126356	0.056361
DP_1	0.245868	0.346582	0.568871	1.694578	0.868568	2.448571
Wavelet	0.148573	0.618584	0.114656	0.565966	0.235724	0.679463

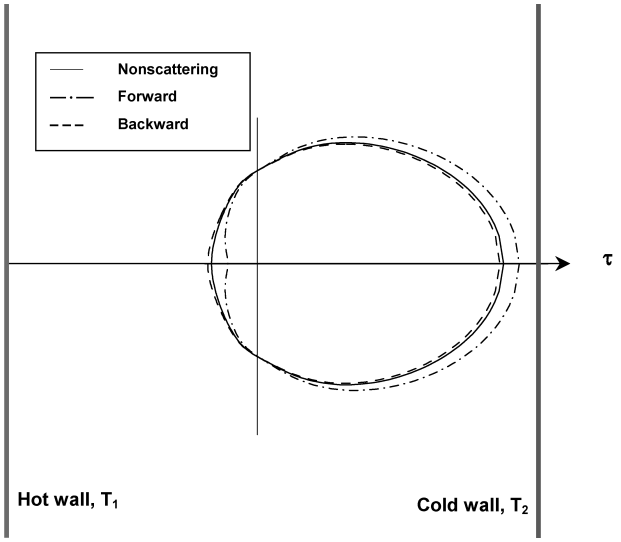

Fig. 2 Angular distribution of the intensity fields at the center of the spatial domain for nonscattering ($\omega = 0$), forward ($\alpha = 1.98398$ and $\omega = 0.5$), and backward ($\alpha = -0.56524$ and $\omega = 0.5$) scattering media ($\tau_L = 1.0$).

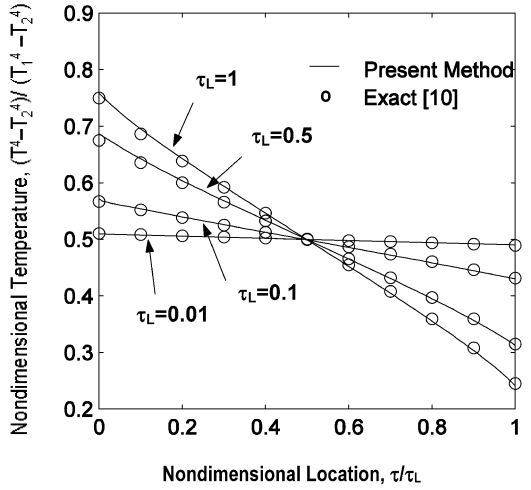

Fig. 3 Comparison of wavelet method and exact solution[10] nondimensional temperature profiles for a nonscattering medium between isothermal plates.

method successfully approximates the angular distribution of the radiative intensity. Figure 3 shows the nondimensional temperature results produced by the wavelet method in the case of nonscattering medium. As seen from Fig. 3, they compare well with exact results.[9]

Figure 4 presents the heat flux distribution corresponding to $\sigma_{SB}T_1^4/\pi = 1$ and $\sigma_{SB}T_2^4/\pi = 0$ and their comparison with the exact solutions[3,12] in the case of a linear anisotropically scattering cold (non-emitting) medium. For the forward scattering medium represented by the scattering phase function coefficient value of $\alpha = 2.319461$, the exact heat flux distribution for the entire domain calculated by using the full phase function is available in the literature.[12] Here, the linear anisotropic function coefficient α is taken as the first term of the full phase function. The exact and the wavelet method results match well through the entire spatial domain. For $\alpha = 0.643833$ and $\alpha = 2.602844$, the heat fluxes are plotted in Fig. 4, and the boundary heat flux values are compared with the exact results.[3] The boundary heat flux results of the wavelet method and of other methods from the literature for these three linear anisotropic function coefficients are also given in Table 1. Table 2 gives the boundary heat flux results for various albedo values ($\omega = 0.2$, 0.5, and 0.8) when $\alpha = 0.643833$. In Tables 1 and 2, the F_9 method

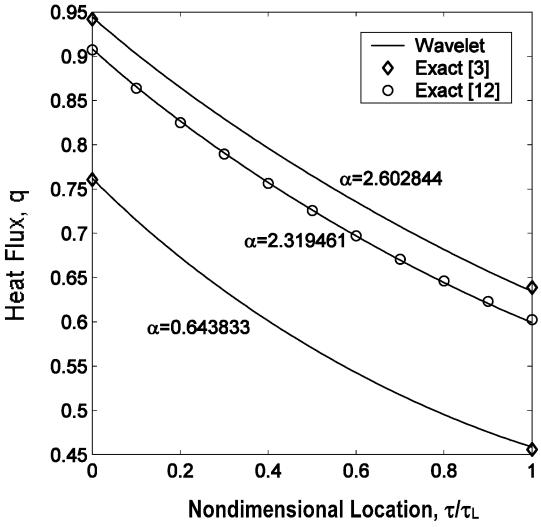

Fig. 4 Comparison of heat flux distributions for three different linear-anisotropic phase functions with exact results[3,12] ($\omega = 0.5$ and $\tau_L = 1.0$).

Table 2 Heat flux comparison: $\tau_L = 1$ and $\alpha = 0.643833$

	Albedo					
	$\omega = 0.2$		$\omega = 0.5$		$\omega = 0.8$	
Methods	$q(0)$	$q(1)$	$q(0)$	$q(1)$	$q(0)$	$q(1)$
F_9 (Exact)	0.96513	0.25397	0.88976	0.32843	0.76057	0.45588
Schuster–Schwarzchil	0.96148	0.17657	0.8791	0.26823	0.74265	0.42256
Two flux	0.96221	0.22271	0.88308	0.31944	0.7574	0.47124
P_1			0.93431	0.31287	0.78743	0.46513
P_3	0.9813	0.24795	0.90095	0.3245	0.7659	0.45636
P_9 (9 term)	0.9678	0.25435	0.89151	0.32884	0.76143	0.45637
DP_1	0.9648	0.2568	0.8889	0.329	0.7587	0.4543
Wavelet	0.9651	0.2513	0.8893	0.3254	0.7588	0.4534
	% Errors compared to exact results					
Schuster–Schwarzchil	0.378187	30.47604	1.198076	18.32963	2.356128	7.308941
Two flux	0.30255	12.30854	0.750764	2.737265	0.416793	3.369308
P_1			5.006968	4.737691	3.531562	2.029043
P_3	1.675422	2.370359	1.257643	1.196602	0.70079	0.105291
P_9 (9 term)	0.276647	0.149624	0.196682	0.124836	0.113073	0.107484
DP_1	0.034192	1.114305	0.096655	0.173553	0.245868	0.346582
Wavelet	0.003108	1.051305	0.051699	0.922571	0.23272	0.544003

Table 3 Effects of spatial variation of the single-scattering albedo $\omega(\tau)$ on reflectance and transmittance; error analysis of wavelets method: exact[4] results

		Forward scattering, $\alpha = 1.98398$		Backward Scattering, $\alpha = -0.56524$	
$\omega(\tau)$	ω_{av}	Reflection	Transmission	Reflection	Transmission
		Linear variation of albedo			
$0.5 + 0.5\tau$	0.5	0.020878	0.386096	0.076146	0.297154
$0.5 + 0.4\tau$	0.5	0.02578	0.384434	0.09003	0.294717
$0.5 + 0.3\tau$	0.5	0.031273	0.383162	0.104754	0.292854
$0.5 + 0.2\tau$	0.5	0.037412	0.3805	0.120375	0.291541
$0.5 + 0.1\tau$	0.5	0.044262	0.381731	0.136961	0.29076
0.5	0.5	0.051899	0.381554	0.154591	0.290501
$0.5 - 0.1\tau$	0.5	0.060408	0.381731	0.173355	0.29076
$0.5 - 0.2\tau$	0.5	0.069889	0.382265	0.193358	0.291541
$0.5 - 0.3\tau$	0.5	0.080458	0.383162	0.214724	0.292854
$0.5 - 0.4\tau$	0.5	0.092248	0.384434	0.237594	0.294717
$0.5 - 0.5\tau$	0.5	0.105416	0.386096	0.262134	0.297154
		Quadratic variation of albedo			
$0.45 + 0.4\tau + 0.15\tau 2$	0.5	0.027872	0.3838	0.094772	0.294892
$0.45 + 0.2\tau + 0.15\tau 2$	0.5	0.039883	0.382881	0.125626	0.291667
$0.45 - 0.2\tau + 0.15\tau 2$	0.5	0.07341	0.382881	0.199941	0.291667
$0.45 - 0.4\tau + 0.15\tau 2$	0.5	0.096499	0.385095	0.245062	0.294892

Table 4 Effects of spatial variation of the single-scattering albedo $\omega(\tau)$ on reflectance and transmission; error analysis of wavelets method: % error of wavelets results

		Forward scattering, $\alpha = 1.98398$		Backward scattering, $\alpha = -0.56524$	
$\omega(\tau)$	ω_{av}	% Error in Reflecion	% Error in Transmission	% Error in Reflection	% Error in Transmission
		Linear variation of albedo			
$0.5 + 0.5\tau$	0.5	8.702941	1.164995	0.724923	0.750116
$0.5 + 0.4\tau$	0.5	6.361521	1.241305	0.394313	0.070576
$0.5 + 0.3\tau$	0.5	4.4831	1.293709	0.116463	0.771033
$0.5 + 0.2\tau$	0.5	2.972308	0.874113	0.097196	0.775877
$0.5 + 0.1\tau$	0.5	1.746419	1.354881	0.262849	0.778993
0.5	0.5	0.745679	1.362848	0.390062	0.780376
$0.5 - 0.1\tau$	0.5	0.067872	1.354881	0.488593	0.778993
$0.5 - 0.2\tau$	0.5	0.724005	1.331799	0.56217	0.775877
$0.5 - 0.3\tau$	0.5	1.240399	1.293709	0.613811	0.771033
$0.5 - 0.4\tau$	0.5	1.629304	1.241045	0.64606	0.764462
$0.5 - 0.5\tau$	0.5	1.921909	1.164995	0.676372	0.750116
		Quadratic variation of albedo			
$0.45 + 0.4\tau + 0.15\tau 2$	0.5	5.195178	0.887441	0.206812	0.761296
$0.45 + 0.2\tau + 0.15\tau 2$	0.5	2.311762	1.308762	0.213332	0.771428
$0.45 - 0.2\tau + 0.15\tau 2$	0.5	0.875902	1.308762	0.599677	0.771428
$0.45 - 0.4\tau + 0.15\tau 2$	0.5	1.629032	1.220738	0.656569	0.761296

represents the exact results. This solution method has the flexibility to handle other scattering phase functions.

The analysis is also applied to a problem where the medium has a spatially varying albedo. Linear and quadratic variations of the albedo are considered. Exact reflectance, $1-q(0)$, and transmittance, $q(1)$, values for both forward ($\alpha = 1.98398$) and backward ($\alpha = -0.56524$) scattering and % errors of the wavelets method results are given in Tables 3 and 4, respectively.

Conclusions

The wavelet method solution to a radiative heat transfer problem involving a one-dimensional plane-parallel linearly anisotropically medium is explained. This method calculates the intensity field at every preselected spatial discrete point as shown in Fig. 2. The temperature distribution and heat flux results are compared with results from existing methods and agree well with the results from the exact solution. It is also shown that method is applicable to problems where albedo varies spatially.

References

[1]Bayazitoglu, Y., and Wang, B. Y., "Wavelets in the Solution of Nongray Radiative Heat Transfer Equation," *Journal of Heat Transfer*, Vol. 120, Feb. 1998, pp. 133–139.

[2]Wang, Y., and Bayazitoglu, Y., "Wavelets and Discrete Ordinates Method in Solving One-Dimensional Nongray Radiation Problem," *International Journal of Heat and Mass Transfer*, Vol. 42, No. 3, 1999, pp. 385–393.

[3]Menguc, M. P., and Iyer, R. K., "Modeling of Radiative Transfer Using Multiple Spherical Harmonics Approximations," *Journal of Quantitative Spectroscopy and Radiative Transfer*, Vol. 39, No. 6, 1988, pp. 445–461.

[4]Cengel, Y. A., and Ozisik, M. N., "Radiation Transfer in an Anisotropically Scattering Plane-Parallel Medium with Space-Dependent Albedo w(x)," *Journal of Quantitative Spectroscopy and Radiative Transfer*, Vol. 34, No. 3, 1985, pp. 263–270.

[5]Fiveland, W. A., "Discrete Ordinate Methods for Radiative Heat Transfer in Isotropically and Anisotropically Scattering Media," *Journal of Heat Transfer*, Vol. 109, Aug. 1987, pp. 809–812.

[6]Daubechies, I., *Ten Lectures on Wavelets*, Society for Industrial and Applied Mathematics, Philadelphia, 1992.

[7]Mallat, S. A., "Theory for Multiresolution Signal Recomposition: The Wavelet Representation," *IEEE Transactions on Pattern Analysis and Machine Intelligence*, Vol. 11, No. 7, 1989, pp. 674–693.

[8]Newland, D. E., *An Introduction to Random Vibrations, Spectral and Wavelet Analysis*, Wiley, New York, 1993, Chap. 17.

[9]Chandrasekhar, S., *Radiative Transfer*, Oxford Univ. Press, London, 1950.

[10]Modest, M. F., *Radiative Heat Transfer*, McGraw–Hill, New York, 1993, Chap. 10.

[11]Miele, A., and Iyer, R. R., "General Technique for Solving Nonlinear, Two-Point Boundary-Value Problems via the Method of Particular Solutions," *Optimization Theory and Applications*, Vol. 5, No. 5, 1970, pp. 382–399.

[12]Felske, J. D., and Kumar, S., "On Computing Radiative Heat Flux Distributions Using the FN Method," *International Journal of Heat and Mass Transfer*, Vol. 29, No. 4, 1986, pp. 635–637.